Please use this PDF proof to check the layout of your article. If you would like any changes to be made to the layout, you can leave instructions in the online proofing interface. First, return to the online proofing interface by clicking "Edit" at the top page, then insert a Comment in the relevant location. Making your changes directly in the online proofing interface is the quickest, easiest way to correct and submit your proof.

Please note that changes made to the article in the online proofing interface will be added to the article before publication, but are not reflected in this PDF proof.

Cell Reports
Physical Science

CellPress
OPEN ACCESS

Article

Single-molecule nanopore dielectrophoretic trapping of α-synuclein with lipid membranes

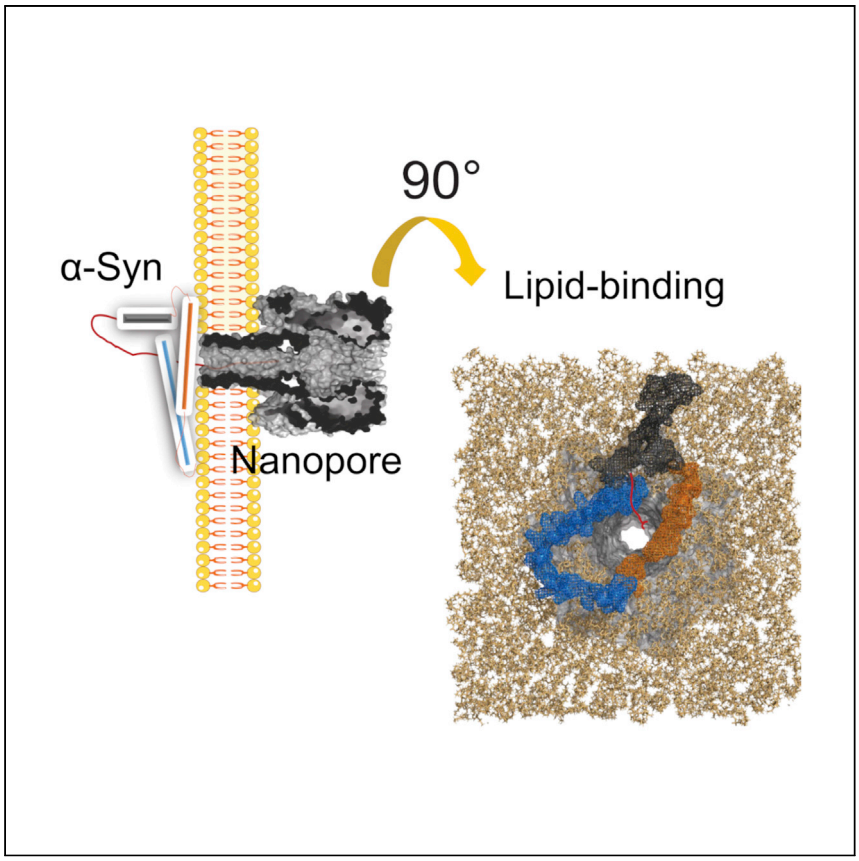

α-Synuclein (α-Syn)-lipid interactions play a crucial role in Parkinson's disease. Wu et al. report that Parkinson's α-Syn in conjunction with a single-strand DNA can be trapped next to the α-hemolysin single nanopore, which provides a method to describe α-Syn lipid-binding and -unbinding kinetics in the presence of the disease-related metal ions or compounds.

Jinming Wu, Tohru Yamashita, Andrew D. Hamilton, Sam Thompson, Jinghui Luo

Jinghui.luo@psi.ch

Highlights

The α-hemolysin nanopore is used to investigate the lipid-binding kinetics of α-synuclein

The binding of the hybridized α-synuclein to lipids can be modulated by Cu^{2+} and Zn^{2+}

α-helix mimetic compound changes the dynamics of α-synuclein in lipid membranes

Wu et al., Cell Reports Physical Science 4, 101243
February 15, 2023
https://doi.org/10.1016/j.xcrp.2022.101243

Please cite this article in press as: Wu et al., Single-molecule nanopore dielectrophoretic trapping of α-synuclein with lipid membranes, Cell Reports Physical Science (2022), https://doi.org/10.1016/j.xcrp.2022.101243

Cell Reports
Physical Science

Article

Single-molecule nanopore dielectrophoretic trapping of α-synuclein with lipid membranes

Q1 Jinming Wu,[1] Tohru Yamashita,[2] Andrew D. Hamilton,[2,3] Sam Thompson,[2,4] and Jinghui Luo[1,5,*]

SUMMARY

The lipid-α-Synuclein (α-Syn) interaction plays a crucial role in the pathogenesis of Parkinson's disease. Here, we investigate the lipid-binding and -unbinding kinetics of α-Syn in an α-hemolysin (αHL) single nanopore. Under an applied voltage, an engineered α-Syn sequence can be trapped at the nanopore due to the dielectrophoretic force. The conformational switch events of α-Syn can be observed at the pore-membrane junction through the interpretation of blockade current amplitudes and dwell time. This allows further analysis of α-Syn conformational dynamics. We study how disease-associated metal ions (Cu^{2+}, Zn^{2+}) modulate the dynamics of α-Syn at the interface of the membranes and pore and how α-helical peptidomimetics stabilize the helical conformation of α-Syn in a lipidic environment. These studies aid our understanding of the complexity of the interaction of α-Syn, lipid membranes, and metal ions, and in using peptidomimetics, a new strategy against α-Syn Q2 **toxicity and aggregation is advanced.**

Q3 Q4 Q5 Q7 Q6

INTRODUCTION

Contributing to the pathogenesis of Parkinson's disease (PD), intrinsically disordered α-Synuclein (α-Syn), a 140-residue protein, is extensively expressed in neurons and enriched in the synaptic cleft.[1] α-Syn consists of three domains: a membrane-binding region with positively charged N-terminal residues from 1 to 60,[2,3] an aggregation associated central hydrophobic domain (NAC: from residues 61–95) and a disordered acidic C-terminal residues from 96 to 140.[4,5] During aging, the protein deposits as β-sheet rich amyloid fibrils,[6] with contemporaneous neuronal dysfunction and degeneration in the brain of PD. Although the biological role of α-Syn remains elusive, a number of studies suggest that it interacts with phospholipid membranes in physiology and pathology, such as synaptic regulation and neuronal death.[6,7] In an effort to reveal the molecular basis of α-Syn toxicity and aggregation, the interaction of α-Syn with membranes has been widely explored.[8–10] Several models have been presented to explain the α-Syn induced toxicity to lipid membranes: (1) membrane-permeabilizing toroidal or barrel pores[11]; (2) carpet model of disrupting and thinning membrane[12,13]; and (3) lipid extraction model.[14] Reciprocally, the lipid membrane affects the binding, misfolding, and aggregation of α-Syn.[15] For instance, α-Syn preferentially binds to membranes with negative charges and high curvatures.[16] α-Syn is also reported to induce lipid expansion and lead to membrane remodeling.[17] In addition, the decreased α-Syn/membrane interaction can facilitate α-Syn aggregation and enhance the neurotoxicity.[18] Folding and unfolding of α-Syn in a lipid membrane environment has been reported to play a vital role in toxicity yet the kinetics remain to be fully explored.[19] It is known that the level of metal ions varies in PD patients and healthy brains.[20,21] For example, the cerebrospinal fluid of the substantia nigra from PD patients has abnormally high concentrations of Cu^{2+}, Fe^{3+}, and Zn^{2+}.[22–24] In addition, metal chelators are able to inhibit the production of α-Syn

[1]Department of Biology and Chemistry, Paul Scherrer Institute, 5232 Villigen, Switzerland

[2]Department of Chemistry, University of Oxford, Oxford OX1 3TA, UK

[3]Department of Chemistry, New York University, New York, NY 10003, USA Q8

[4]Department of Chemistry, University of Southampton, Southampton SO17 1BJ, UK

[5]Lead contact

*Correspondence: Jinghui.luo@psi.ch

https://doi.org/10.1016/j.xcrp.2022.101243

Please cite this article in press as: Wu et al., Single-molecule nanopore dielectrophoretic trapping of α-synuclein with lipid membranes, Cell Reports Physical Science (2022), https://doi.org/10.1016/j.xcrp.2022.101243

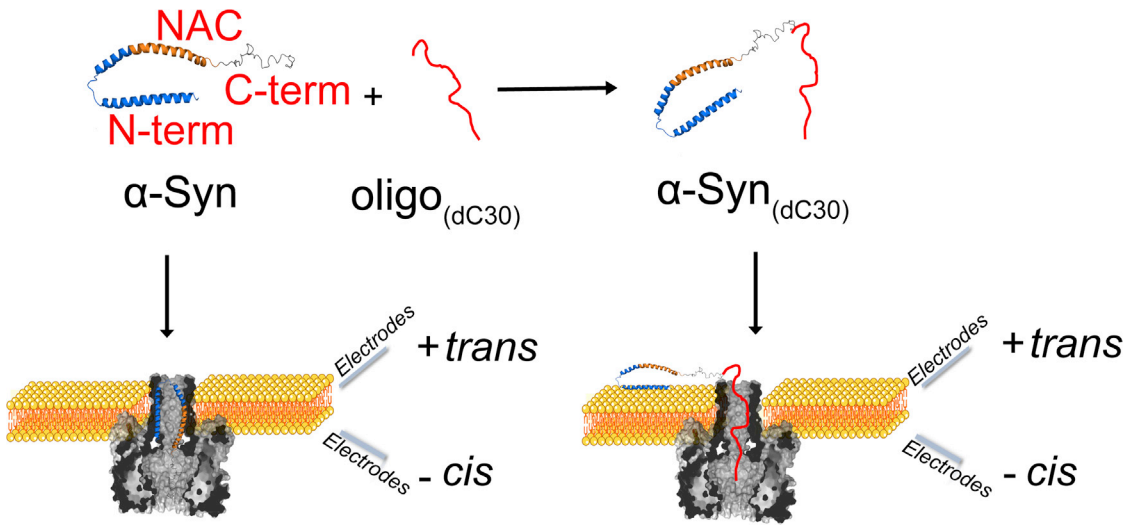

Figure 1. Illustration of α-Syn-membrane interactions studied by single-molecule nanopore analysis

Wild-type (WT) α-Syn was added to the *trans* side of a single α-hemolysin (αHL) nanopore and induced the blockage of the αHL channel in a lipid bilayer. To study the interaction of full-length α-Syn with the lipid membrane, α-Syn mutant (A140C) was covalently linked to oligonucleotide dC30. To hybridize α-Syn with single-stranded dC30, 2,2′-dipyridyldisulfide was used to activate 5′-thiol (hexamethylene linker)-modified oligo(dC)30 for forming the covalent bond with the cysteine from the α-Syn mutant (A140C). The conjuncted $\alpha\text{-Syn}_{(dC30)}$ was then added to the *trans* side of the αHL nanopore and induced the dielectrophoresis trapping of $\alpha\text{-Syn}_{(dC30)}$ in lipid membranes. With the applied voltage, the highly charged oligo(dC30) acted as a leading sequence to thread into the pore and the α-Syn part remained on the *trans* side for the interaction with lipid membranes. To minimize the effect of terminal modification on the interaction, the none-lipid active C terminus of α-Syn was implemented as the conjunction site, and the N-terminal and NAC domains of α-Syn remained flexible for the interaction with lipid membranes.

oligomer-induced reactive oxygen species and meanwhile prevent oligomer-induced neuronal death.[25] It suggests that metal ions also act as an important factor to modulate α-Syn folding, aggregation, and neurotoxicity.[26] Overall, both the metal ions and lipid membrane interaction with α-Syn are two main factors that are involved in the pathogenesis of PD, either in a direct causal manner or as a consequence of misfolding. Thus, it is important to investigate how metal ions modulate the α-Syn binding and unbinding to the lipid membranes for further understanding of the molecular mechanisms of α-Syn in the pathology of PD.

Single-nanopore technologies have been used to record the interaction or aggregation among amyloid proteins with or without metal ions or small molecules at the single-molecule level.[27–30] The recording is on the basis of individual amyloid proteins blocking or translocating through a single nanopore. The dwell time and residual current of single-nanopore transient blockade by individual amyloid proteins can be extracted to gain an understanding of protein folding, topology, and noncovalent interactions of the lumen in the nanopore.[31,32] A biological nanopore, such as an α-hemolysin (αHL) nanopore, is an assembly of pore-forming toxins in reconstituted lipid membranes across *cis* (ground side) and *trans* sides (Figure 1). Secreted by *Staphylococcus aureus*, αHL oligomerizes and self-assembles into a heptameric mushroom-shaped β-barrel pore.[33] By adding the amyloid peptides into the *cis*-side of wild-type αHL, Wang et al. investigated how amyloid proteins block or translocate the single nanopore for the characterization of amyloid aggregation or interaction.[28,29] As αHL pore entry (which is *cis*-side in our convention) is elevated ~5 nm above the bilayer, the *trans*-entrance (αHL exit) of the channel lies close to the bilayer surface. Proteins, especially those preferring to interact with membranes like α-Syn from the *trans* side,[34] easily enter the channel. After the addition of α-Syn into the *trans* side, Gurnev et al. observed the membrane-binding α-Syn, of which the

Please cite this article in press as: Wu et al., Single-molecule nanopore dielectrophoretic trapping of α-synuclein with lipid membranes, Cell Reports Physical Science (2022), https://doi.org/10.1016/j.xcrp.2022.101243

C-terminal tail entered the pore and the N and NAC domains partitioned on the surface of the lipid membrane.[10] Tavassoly et al. used the same setup and found that Cu^{2+} ions induce large conformational changes of α-Syn.[35] However, in these cases, it is unclear how the whole sequence of α-Syn interacts with the lipid membranes and how metal ions regulate the entire α-Syn binding and unbinding to lipid membranes. Recently, Rodriguez-Larrea et al. studied the unfolding kinetics of thioredoxin (Trx) in a conjunction with a DNA oligonucleotide leader oligo(dC30) through a nanopore.[36,37] The oligo(dC30) linked Trx was added to the *cis* part of the chamber, where the unfolding of Trx only occurred without interacting with lipid membranes. Their work provides an insight into the unfolding kinetics of Trx without interacting with lipid membranes. The dynamics of α-Syn in a lipid membrane environment play a vital role in toxicity yet the kinetics remain to be fully explored.

Using single-nanopore analysis, we investigated how Cu^{2+} and Zn^{2+} modulates α-Syn dynamic, lipid-binding and -unbinding states on the *trans* side that has a lipidic environment at the single-molecule level as shown in Figure 1. By the conjunction of α-Syn mutant (A140C) with oligo(dC30), we observed two stepwise blockades of single-nanopore by the oligo-linked α-Syn, which may be explained by single-nanopore dielectrophoresis (DEP) force model.[38] In this model, the observed two blockade levels were caused by its interaction with the lipid membrane and trapped by a strong DEP force at the pore-membrane junction. We further studied two metal ions, Cu^{2+}, Zn^{2+}, and a helix mimetic compound that modulates α-Syn dynamics in a lipidic environment. These studies seek insights into the complexity of α-Syn interactions with lipid membranes in the presence of metal ions and small molecule modulators of misfolding, thus allowing the development of new strategies against α-Syn toxicity and aggregation.

RESULTS AND DISCUSSION

Design of membrane model

To investigate whether the PD-associated Cu^{2+} ions and Zn^{2+} ions modulate the binding between the lipid bilayer and α-Syn, we conducted a single-molecule αHL nanopore electrical recording in the presence of α-Syn with or without Cu^{2+} ions, shown in Figure 1. The αHL nanopore was reconstituted in a planar lipid bilayer, composed of a mixture of neutrally charged DOPC (1,2-dioleoyl-sn-glycero-3-phosphocholine) and negatively charged DOPG (1,2-dioleoyl-sn-glycero-3-phospho-(1′-rac-glycerol)) at a ratio of 4:1. Though α-Syn is negatively charged (+3 net charge of N-terminus and −8 net charge of C terminus), it is generally accepted that it is the N-terminus that modulates α-Syn interaction with membranes, while the C terminus remains unbound.[39] In addition, α-Syn preferentially binds to more physiologically relevant lipids (bilayer or small unilamellar vesicles) with anionic headgroups like PG,[40] which typically takes up less than 30% of lipids and has been used as a model lipid in the study of peptides with membrane-driven association,[41,42] cell-penetrating,[43–45] and the channel activities.[46] Thus, the mixture of DOPC:DOPG (4:1) is chosen in our setup to study the interaction of α-Syn with lipid membranes.

It has been reported that no blockage event for wild-type (WT) α-Syn in the αHL nanopore is observed[10,29] when the voltage is lower than 40 mV. Here, we applied the potential between the lipid bilayer −100 mV due to the easy observation of the full blocked capture of WT α-Syn in the αHL nanopore.[29] In addition, higher voltage makes current interruptions easily discernible. α-Syn binding to channels has also been demonstrated to vary with the bulk salt concentration.[10] The higher salt concentration makes the capture by the channel easier, due to the decreased Coulomb and/or solvation barriers by high salt concentrations, in which these barriers are

Please cite this article in press as: Wu et al., Single-molecule nanopore dielectrophoretic trapping of α-synuclein with lipid membranes, Cell Reports Physical Science (2022), https://doi.org/10.1016/j.xcrp.2022.101243

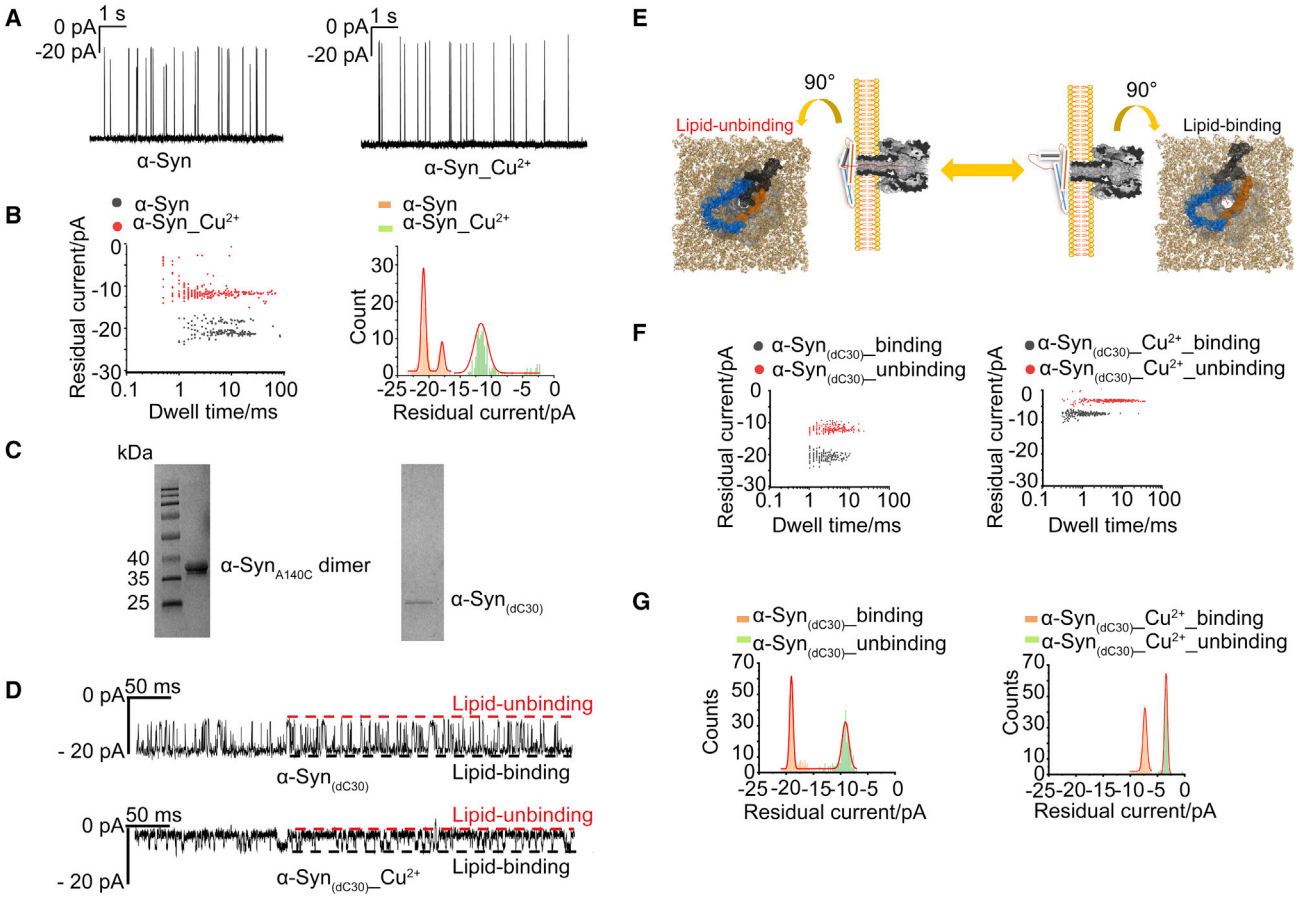

Figure 2. Interaction of full-length α-Syn with lipid membranes

(A) Representative current traces reveal the translocation of wild-type (WT) α-Syn through a single αHL nanopore in the presence or absence of Cu^{2+} ions with the applied voltage of −100 mV. The samples were added to the *trans* side of the lipid bilayer, composed of DOPC and DOPG (4:1).

(B) Left: scatter distribution of the event dwell time plotted against the residual current in the presence of WT α-Syn with or without Cu^{2+} ions. Right: residual current histogram in the presence of WT α-Syn with or without Cu^{2+} ions (originated from $CuCl_2$.).

(C) The conjunction of α-Syn (A140C) with single-strand DNA oligos (dC30) through pyridyl disulfide reaction (left) and α-Syn (A140C) dimer.

(D) Representative current recording of a single αHL nanopore across a planar lipid bilayer composed of DOPC and DOPG (4:1) in the presence of $α\text{-Syn}_{(dC30)}$ with or without Cu^{2+} at −100 mV (upper).

(E) Illustration of α-Syn conformational switch in lipid membranes. α-Syn binding to lipid membranes accompanies the higher residual current.

(F) Scatter distribution of the event dwell time plotted against the residual current in the presence of $α\text{-Syn}_{(dC30)}$ with or without Cu^{2+} ions. Due to the nanopore dielectrophoresis trapping, $α\text{-Syn}_{(dC30)}$ binding to the lipid bilayer generated a higher residual current than the unbinding state. Two distinct events were classified, the lipid-unbinding (red scatters) and lipid-binding events (black scatters) of $α\text{-Syn}_{(dC30)}$.

(G) Residual current histogram in the presence of $α\text{-Syn}_{(dC30)}$ with or without Cu^{2+} ions. Similar to the presence of WT α-Syn, the addition of Cu^{2+} ions to the hybrid α-Syn reduced the residual current of electrical recording, suggesting the different α-Syn conformations in the presence of Cu^{2+} ions. For all the nanopore experiments, the two sides of the chamber (*cis* and *trans*) are filled with 10 mM HEPES buffer, pH 7.4, with 1 M KCl. The final concentration of WT or hybridized $α\text{-Syn}_{(dC30)}$ and Cu^{2+} is 0.2 μM and 5 μM, respectively.

suggested to control the rate of α-Syn binding to channels. We fixed the salt concentration at 1 M, which is a standard salt concentration that has been applied in several publications.[47–51] Figure 2A shows transient blockade events of the α-Syn without and with Cu^{2+} from the *trans* side, which is consistent with the previous observation that α-Syn causes transient nanopore blockage.[29] The final concentration of Cu^{2+} is 5 μM in our studies, far from the concentration of 0.3 mM below which Cu^{2+} does not change the architecture of αHL nanopore and keeps the current steady.[52] The stoichiometric ratio of 1:25 for α-Syn to Cu^{2+} was designed based on the previous publication.[35] At this ratio, Cu^{2+} induces α-Syn to a more folding and compact structure.[35] In the presence of Cu^{2+}, α-Syn induces lower residual currents, which are

Please cite this article in press as: Wu et al., Single-molecule nanopore dielectrophoretic trapping of α-synuclein with lipid membranes, Cell Reports Physical Science (2022), https://doi.org/10.1016/j.xcrp.2022.101243

shown as the red scatter distribution in Figure 2B. The histogram analysis of the residual current amplitudes estimates α-Syn with and without Cu^{2+} ions to be −21 pA and −11.5 pA, respectively. The lower nanopore blockage induced by the addition of Cu^{2+} ions revealed a more folded structure of α-Syn. This result is consistent with the previous publication that Cu^{2+} can induce the more α-helical signal of α-Syn in the presence of lipid vesicles.[53] The transient nanopore blockage may be caused by the translocation of α-Syn to the *cis*-side.[10] The charged C terminus of α-Syn presumably leads the translocation of the full-length protein into the lumen of the nanopore. When the C terminus enters the lumen, the current changes can be mainly attributed to the bilayer interaction with the N-terminus rather than the full-length protein. However, the transient current signal does not provide informative biophysical characterization for single-molecule α-Syn interaction with a lipid membrane.

Interaction of full-length α-Syn with lipid membranes

To gain insights into the interaction of full-length α-Syn with lipid membranes, we linked the mutated α-Syn(A140C) to a single-strand 5′-thiol-modified DNA oligonucleotide dC30 with a hexamethylene linker that was activated with 2,2′-dipyridyl disulfide to yield 5′-S-thiopyridyl oligonucleotides for coupling to α-Syn(A140C) (Figure S3B).[36] Since α-Syn(A140C) only has one cysteine residue replacing alanine 140, dC30 is coupled to the terminal cysteine residue (C140). In this reaction, α-Syn(A140C) can be dimerized through cysteine-cysteine (that is S-S) linkage as described in the method part. We fractionated hybrid α-Syn(A140C)-dC30 (abbreviation $\alpha\text{-Syn}_{(dC30)}$) and α-Syn dimer by ionic exchange column and confirmed $\alpha\text{-Syn}_{(dC30)}$ and αSyn dimer bands on the SDS-gel page (Figure 2C). The purpose of oligo(dC30) is used as a leading to thread into the αHL pore.[36,47,54] When applying a negative potential at the *trans* side, the negative-charged oligonucleotides dC30 in the *trans* part will remain α-Syn on the lipid membranes. Also, the N-terminal and NAC domains of α-Syn interact with membranes.[39] In this scenario, the dC30 will get trapped in the nanopore under the applied voltage due to the α-Syn N-terminal interaction with the lipid membranes. The trapped dC30 does not affect α-Syn conformation and interaction, especially the interaction with lipids. The interaction can remain the protein away from the translocation into the nanopore and trap the single protein for understanding their interaction kinetics with lipids. The shorter oligo-nucleotides will be more difficult to control their passing through the nanopore due to the high-speed translocation and insufficient dwell time to reach analytic resolution.[55] The oligonucleotide dC30 was chosen instead of dA30 or dT30, mainly due to poly(dC) giving a better discernible signal than poly(dA)[55] and longer duration times of dC than that of dT.[56] The purification of hybrid $\alpha\text{-Syn}_{(dC30)}$ was shown on SDS-PAGE in Figure 2C. The addition of $\alpha\text{-Syn}_{(dC30)}$ to the *trans* side caused the trapping of αHL nanopore in Figure 2D. This may be attributed to two factors: (1) $\alpha\text{-Syn}_{(dC30)}$ released the full-length α-Syn for the interaction with the head group of lipid membranes; (2) with its longer sequence, $\alpha\text{-Syn}_{(dC30)}$ had a stronger dielectrophoretic force (DEP) at the nanopore conjunction than the WT. DEP trapping was observed in a previous study where α-Syn could be trapped in the constriction of a nanopore and was considered as a reservoir-microchannel junction.[29] Here, we observed two distinguished trapping levels in Figures 2D–2G, with approximately 10 pA current difference in the presence of $\alpha\text{-Syn}_{(dC30)}$ but not WT α-Syn. At a nanopore conjunction, a DEP of the opposite electric field induces particle deflection, focusing, and trapping.[38] Large complexes, like $\alpha\text{-Syn}_{(dC30)}$, can be trapped in the conjunction, but the smaller WT α-Syn translocates through the nanopore. Two different trapping events can be induced by the α-Syn interaction with the lipid surface and a DEP that contributed to the binding and unbinding of α-Syn to the

lipid membranes (Figure 2E). The lower residual current we observed is assumed to be due to the folding of α-Syn.

With the applied voltage, the single-strand DNA, oligo(dC30), leads the folded α-Syn protein away from the lipid membrane and blocks the nanopore. The dwell time that α-Syn trapped in the pore with the low residual currents is $t_{m\_unbinding}$. The time that α-Syn remained in the lipid-binding conformation with the high residual currents is $t_{m\_binding}$. The high residual currents represent less blockage of the nanopore by oligo(dC30)-linked-α-Syn because of the unfolded α-Syn protein interaction with the lipid membrane on the *trans* side. We refer it to the lipid-binding level here. The two repeated levels of the low and high residual currents (lipid-unbinding and lipid-binding) suggest that the engineered α-Syn might have a kinetic equilibrium between lipid-unbinding and lipid-binding conformations. Thus, $t_{m\_binding}$ was calculated from the interevent interval of two lipid-unbinding levels. The higher $t_{m\_binding}$ we observed, the longer α-Syn stayed in the lipid-binding conformation in Figure 2E. The dynamics and kinetics could be modulated by metal ions or small molecule ligands. For instance, as shown in Figure 2D, the inverted signal in the presence of Cu^{2+} ions represents more blockage by an α-Syn complex with Cu^{2+}. Cu^{2+} ions refolded α-Syn in a more compacted structure with the reduced residual current and longer dwell time in the electrical recording in Figures 2F and 2G. Analysis of these trapping events offers insights into the conformational dynamics and kinetics of α-Syn in the presence of lipid membranes, metal ions, and aggregation inhibitors.

As a control, we investigated the conformational dynamics of $\alpha\text{-Syn}_{(dC30)}$ in the presence of a neutrally charged lipid membrane, composed of DPhPC (1,2-diphytanoyl-sn-glycero-3-phosphocholine). Figure 3A shows that α-Syn displays fewer binding and unbinding events in DPhPC lipids than that in negatively charged DOPC:DOPG (4:1) lipid membranes (Figure 2D), suggesting less completely α-Syn trapping into the nanopore. This may be explained by the greater association of α-Syn with a negatively charged lipid membrane, in agreement with previous studies.[57–59] Similar to the presence of a negatively charged lipid membrane, the addition of Cu^{2+} ions and the hybridized α-Syn to the neutrally charged lipid membrane gave reduced residual current in the electrical recording. This reveals both Cu^{2+} ions and the nature of the lipid determine the conformation of α-Syn.

Effect of metal ions on lipid-binding and -unbinding events

An increased dielectrophoretic force was carried out for studying different trapping events. We increased the voltage to −200 mV and observed in Figure 4A that the trapping events are similar to the recording at −100 mV in Figure 2D. However, the presence of Cu^{2+} ions slightly changes the effect of trapping at −200 mV in Figure 4A, in comparison to the trapping at −100 mV. It suggests a higher voltage may give a stronger dielectrophoretic force for the trapping and interaction of the α-Syn moiety with the lipid membranes in the presence of Cu^{2+} ions. A plausible explanation is that α-Syn forms a folded complex with Cu^{2+} ions, taking a stronger dielectrophoretic force at a higher voltage. We compared the modulation of the α-Syn interaction with lipid membranes in the presence of Cu^{2+} and Zn^{2+} at −200 mV. Since the lowest blockade current is observed with Cu^{2+}, this suggests a more compacted α-Syn conformation. Likewise, the lipid-unbinding time constant (τ_1) is higher with Cu^{2+} than Zn^{2+} (Table 1), suggesting Cu^{2+} forms a more stable complex with α-Syn in the lipid membrane. This result is consistent with the outcome from ESI-IM-MS method that Cu^{2+} induced a more compact α-Syn conformation when Cu^{2+} binds to α-Syn *in vitro*.[60] In the presence of the Cu^{2+} ions, we observed a higher $t_{m\_binding}$ value compared with that of α-Syn alone as shown in Table 1. This indicates

Please cite this article in press as: Wu et al., Single-molecule nanopore dielectrophoretic trapping of α-synuclein with lipid membranes, Cell Reports Physical Science (2022), https://doi.org/10.1016/j.xcrp.2022.101243

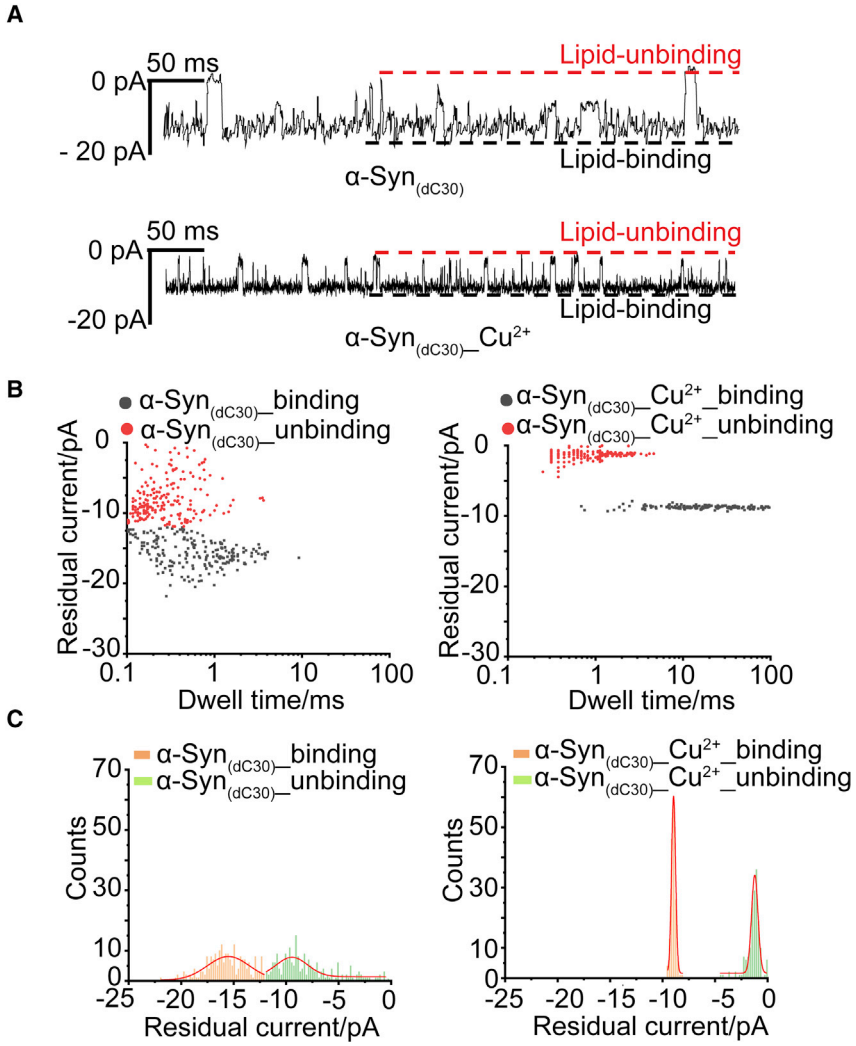

Figure 3. Lipid-binding and unbinding events of α-Syn$_{(dC30)}$ in a neutrally charged lipid membrane

(A) Representative current recording of hybridized α-Syn$_{(dC30)}$ with or without Cu^{2+} translocating a single αHL nanopore on the neutrally charged DPhPC lipid bilayer at −100 mV. Two distinct conformational switch events of α-Syn$_{(dC30)}$ were classified. The unbinding α-Syn$_{(dC30)}$ to lipid membranes induced a smaller residual current than the binding conformation. The final concentration of hybridized α-Syn$_{(dC30)}$ and Cu^{2+} is 0.2 μM and 5 μM respectively. 10 mM HEPES buffer, pH 7.4, with 1 M KCl was used to fill the two compartments of the chamber (*cis* and *trans*).

(B) Scatter distribution of the dwell time plotted against the residual current of α-Syn$_{(dC30)}$ with or without Cu^{2+}. The red and black scatters represent the lipid-unbinding and binding events, respectively.

(C) Distributions of residual current of α-Syn$_{(dC30)}$ with or without Cu^{2+} are plotted as histograms, fitting with the multiple-peak Gaussian function.

that the Cu^{2+} ions keep longer the interaction of α-Syn structures with the lipid membrane. We assumed that α-Syn forms a compacted and folded structure in the presence of Cu^{2+}. Such compacted α-Syn conformation takes a longer time for each trapping event during the equilibrium. Though Zn^{2+} induced a longer $t_{m\_binding}$ compared with Cu^{2+}, Zn^{2+} did not show a lower residual current at the lipid-unbinding level, suggesting that Zn^{2+} and α-Syn form a less compacted conformation than that of Cu^{2+} and α-Syn. A plausible explanation is that Zn^{2+} induced different α-Syn conformation changes from Cu^{2+}. The addition of Zn^{2+} causes longer time for α-Syn

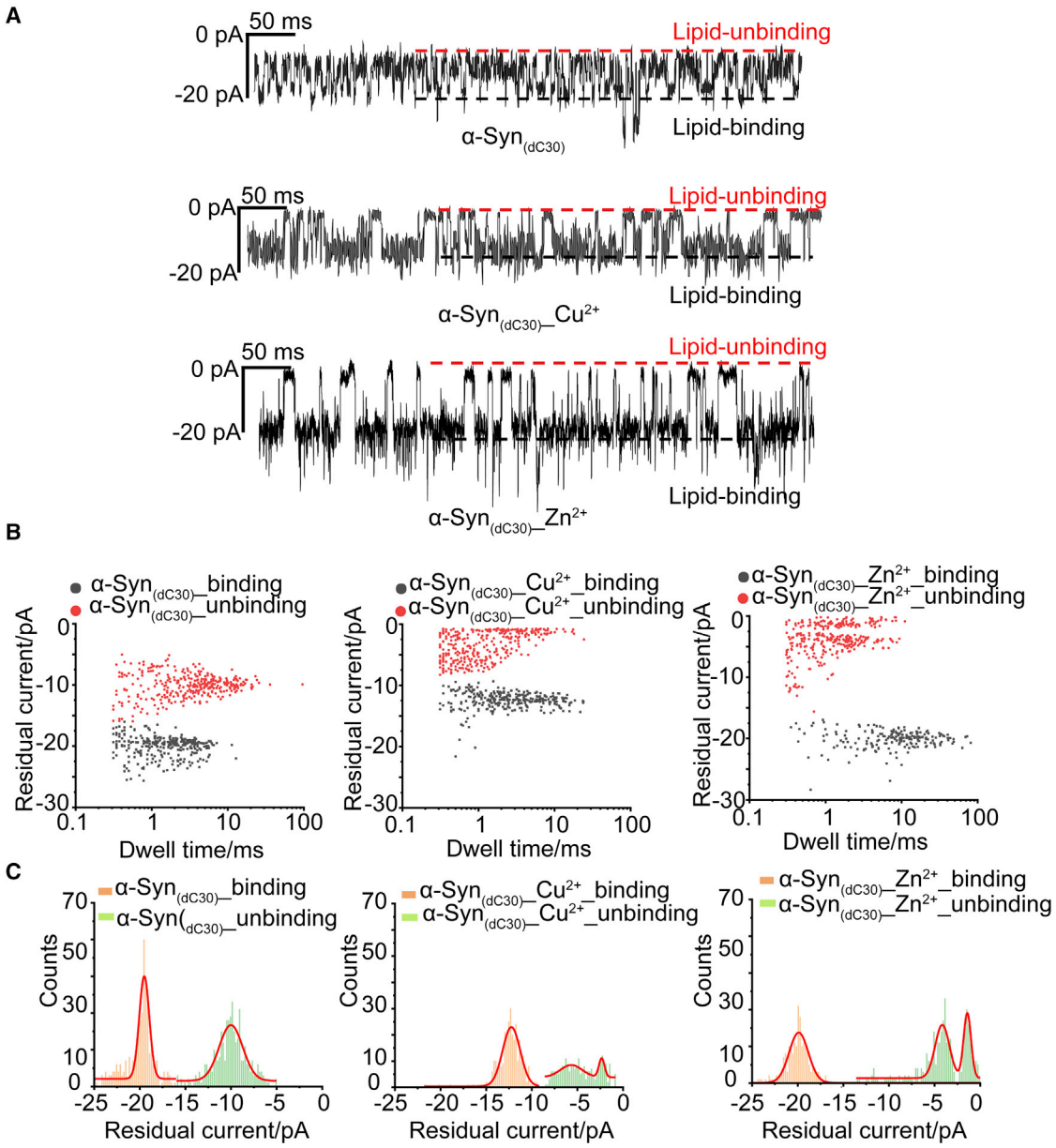

Figure 4. Lipid-binding and unbinding events of α-Syn$_{(dC30)}$ in the presence of different metal ions

(A) Representative current recording of hybridized α-Syn$_{(dC30)}$ with or without Cu^{2+} or Zn^{2+} translocating a single αHL nanopore on the negatively charged DOPC:DOPG (4:1) lipid bilayer at −200 mV. Two distinct conformational switch events of α-Syn$_{(dC30)}$ were classified. The unbinding α-Syn$_{(dC30)}$ to lipid bilayers induced less blocked current than the binding structure. The final concentration of hybridized α-Syn$_{(dC30)}$ and Cu^{2+} or Zn^{2+} is 0.2 μM and 5 μM, respectively. The experiments were conducted with 10 mM HEPES buffer, pH 7.4, with 1 M KCl.

(B) Scatter distribution of the dwell time plotted against the residual current of α-Syn$_{(dC30)}$ with or without Cu^{2+} or Zn^{2+}. The red and black scatters represent the unbinding and binding events, respectively.

(C) Distribution of residual current of α-Syn$_{(dC30)}$ with or without Cu^{2+} or Zn^{2+} are plotted as histograms, fitting with the multiple-peak Gaussian function. The metal ions Cu^{2+} and Zn^{2+} are obtained from $CuCl_2$ and $ZnSO_4$, respectively.

switch between the lipid-binding and lipid-unbinding conformations. Our trapping method as a complementary technique allows observing the dynamics of α-Syn binding to lipid membranes in the presence and absence of the disease-related metal ions. The residual current and time constant provide insight into the folding and complex stability information of metal ions, α-Syn, and lipid membranes.

Please cite this article in press as: Wu et al., Single-molecule nanopore dielectrophoretic trapping of α-synuclein with lipid membranes, Cell Reports Physical Science (2022), https://doi.org/10.1016/j.xcrp.2022.101243

Table 1. Conformational switch events of α-Syn$_{(dC30)}$ with or without Cu^{2+} on DOPC:DOPG (4:1) lipid bilayer at −200 mV

	α-Syn$_{(dC30)}$	α-Syn$_{(dC30)}$_Cu^{2+}	α-Syn$_{(dC30)}$_Zn^{2+}
$\tau_{1\_unbinding}$ (ms)	0.623 ± 0.266	1.29 ± 0.201	0.68 ± 0.025
$\tau_{2\_binding}$ (ms)	0.515 ± 0.097	1.80 ± 0.119	4.537 ± 0.134
$K_{on\_unbinding}$ ($L \cdot ms^{-1} \cdot g^{-1}$)	1.60×10^6	1.94×10^6	1.47×10^6
$K_{on\_binding}$ ($L \cdot ms^{-1} \cdot g^{-1}$)	7.750×10^5	5.56×10^5	2.20×10^5
$t_{m\_unbinding}$ (ms)	6.047 ± 0.866	2.12 ± 0.158	1.85 ± 0.10
$t_{m\_binding}$ (ms)	2.108 ± 0.100	4.106 ± 0.25	12.82 ± 0.87

The time constant $\tau_{1\_lipid\text{-}unbinding}$ and $\tau_{2\_lipid\text{-}binding}$ were calculated from the scatter distribution of the dwell time against the residual current, which was fitted by the double-exponential decay function. The rate constant is $K_{on} = 1/[\tau_{on} \times C_{peptide}]$. t_m represents the mean value of the dwell time.[15] $C_{peptide}$ represents the final concentration of the testing peptide in the aqueous phase.

The single-nanopore trapping technique was further applied to investigate how small molecules, which can disrupt amyloid protein fibrillization kinetics, modulate α-Syn conformation in the presence of a lipid membrane (Figure 5). Compound **3**, an α-helical mimetic compound that can imitate the topography of an α-helix, is functionalized with, at physiological pH, cationic NH_3^+, anionic COO^-, and branched alkyl groups in the *i*, *i+4*, and *i+7* positions, respectively (Figure 5B).[61] Mimetic **3** is designed to target the helical surface of α-Syn comprising three amino acids (negatively charged Glu,[46] positively charged His,[50] and hydrophobic Ala[53]) that occupy the *i*, *i + 4*, and *i + 7* positions (Figure 5A), by forming complementary contacts. The side chain of His50 includes the ionizable imidazole ring with a pKa value of 6.78.[62] The lipidic environment can cause the pKa shift of His50 to 7.7.[62] In the lipidic environment of our experimental condition, His50 is supposed to be positively charged for interacting with anionic group at i+4 in Figure 5. Thus, the acid form of His50 of α-Syn can bind to i+4 (anionic) position of mimetic 3 compound at pH 7.4 via the electrostatic interaction. We have previously successfully demonstrated such an approach with islet amyloid polypeptide.[63] As shown in Figure 5C, compared with α-Syn$_{(dC30)}$ alone, the conformational switch events of α-Syn in the presence of mimetic **3** in lipid membranes are significantly reduced, consistent with the stabilization of the helical protein. Besides peptidomimetic **3**, dopamine, another compound that kinetically stabilizes α-Syn oligomers,[64–67] also reduces the binding and unbinding events of α-Syn to lipid membranes, but with more spikes and greater residual current, indicative of the weaker binding of dopamine to α-Syn than that of mimetic **3**. These results suggest single-nanopore trapping is a suitable method to characterize the effect small molecules exert on α-Syn conformational dynamics in the presence of lipid membranes. Moreover, it may find use as a primary tool for the screening and optimization of aggregation inhibitors.

Previously, single-nanopore studies characterized the conformation and dynamics of amyloid proteins using several heterogeneous events rather than the kinetics of a single-molecule amyloid protein. Here we observed the α-Syn interaction with lipids at a single-molecule level by trapping the molecule under externally applied dielectrophoretic force. We show that the conformational switch kinetics of α-Syn in the presence of lipid membranes can be extracted from single-molecule nanopore dielectrophoretic trapping. The binding and unbinding of α-Syn are modulated by the charged nature of the lipids constituting the membranes and the metal ions. Therefore, the nanopore trapping method offers a single-molecule detection for understanding the kinetic conformation switch of intrinsically disordered proteins in a lipidic environment.

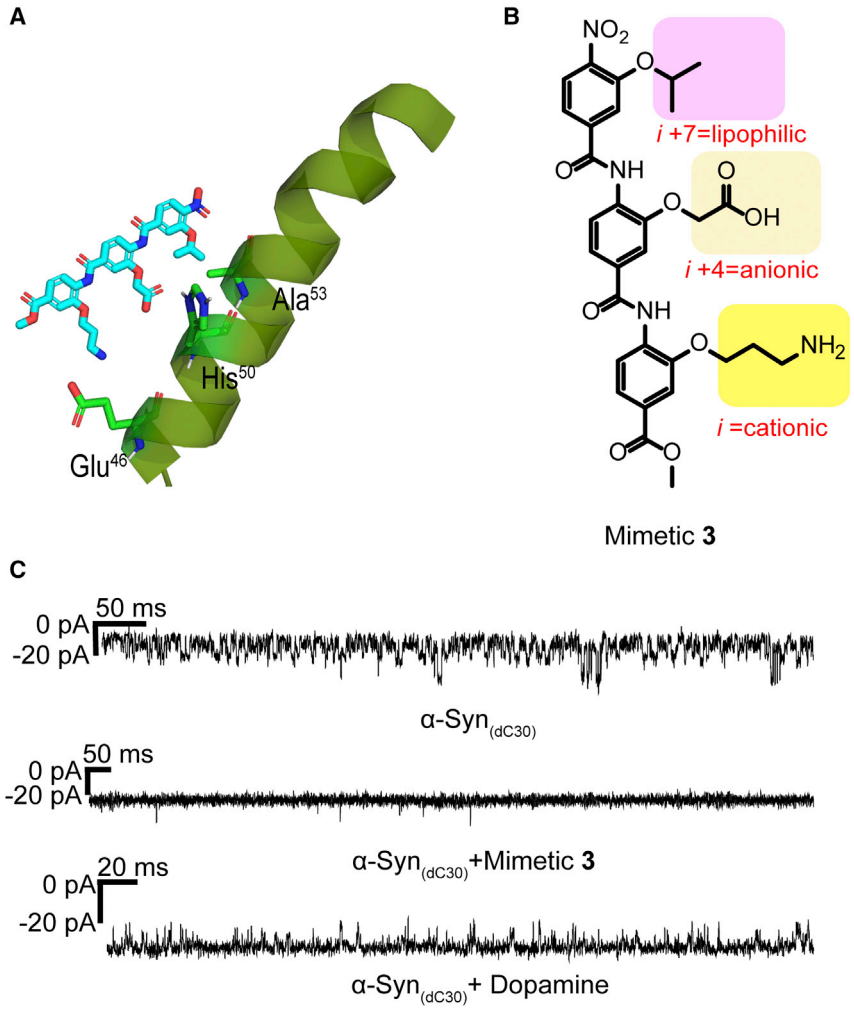

Figure 5. Conformational switch events of α-Syn$_{(dC30)}$ in the presence of small molecules

(A) Schematic representation of an α-helix mimetic compound interacting with three residues (Glu,[46] His,[50] and Ala[53]) located in the α-helical region of membrane-bound α-Syn.

(B) Structure of α-helix mimetic compound 3 with three side chains (yellow, orange, and pink highlights) designed to form complementary contacts with residues Glu,[46] His,[50] and Ala[53] through salt bridges at *i* and *i+4*, and hydrophobic interactions at *i+7*.

(C) Representative current recordings of hybridized α-Syn$_{(dC30)}$ in the presence of mimetic 3 or dopamine. Negatively charged DOPC:DOPG (4:1) lipid bilayer was formed under the voltage of −200 mV. The two *cis* and *trans* sides were filled with 10 mM HEPES buffer, pH 7.4, with 1 M KCl.

The limitations of our study are that binding and unbinding characteristics of trapping for hybridized α-Syn are under externally applied dielectrophoretic force. The external force and hybridization may influence the intrinsic structural properties of α-Syn in a lipidic environment. To address these issues future work in our laboratory will explore the use of electrode-free nanopore sensing.[68] Additionally, the single-nanopore technique in our study still remains challenging to visualize the dynamics and kinetics of α-Syn, in which direct imaging would be more straightforward to validate these two conformational states at a single-molecule level. The combination of fluorescence-based diffusion method would be one potential method to observe the different status of molecules through the fluorescence signal changes,[68] though the further work will be explored in our lab.

Please cite this article in press as: Wu et al., Single-molecule nanopore dielectrophoretic trapping of α-synuclein with lipid membranes, Cell Reports Physical Science (2022), https://doi.org/10.1016/j.xcrp.2022.101243

Last, we found that disease-associated metal ions and peptidomimetic compounds modulate the conformational dynamics of α-Syn in lipid membranes. In principle, the method can be used for screening inhibitors suppressing the interaction between lipid and α-Syn, which will be the subject of further study. The development of microelectrode-cavity arrays, such as the commercial Orbit 16 TC equipped with the dedicated low-noise 16-channel amplifier, allows the formation of 16 selected ion-conducting channels or pores in parallel.[69] We believe that further parallelization of single-molecule nanopore trapping has the potential to enable high-throughput screening of potential therapeutics against intrinsically disordered proteins in lipidic environments.

EXPERIMENTAL PROCEDURES

Resource availability

Lead contact

Further information and requests for reagents and resources are available from the lead contact, Jinghui Luo (Jinghui.luo@psi.ch).

Materials availability

All materials mentioned in this study can be made available upon reasonable request to the lead contact.

Data and code availability

All data reported in this article can be made available from the lead contact upon reasonable request.

Supporting information

The experimental section (Materials and methods) and Figures S1–S9 are available in supplemental information.

SUPPLEMENTAL INFORMATION

Supplemental information can be found online at https://doi.org/10.1016/j.xcrp.2022.101243.

ACKNOWLEDGMENTS

We acknowledge financial support from The Universities of Oxford and Southampton, the Paul Scherrer Institute, the EPSRC (EP/S028722/1 to S.T.), the Swiss National Scientific Foundation (310030_197626 to J.L.), the BrightFocus Foundation (A20201759S to J.L.), and Takeda Pharmaceutical Company Limited for their generosity in providing financial and logistical support during a sabbatical position for T.Y. as a visiting scientist at the University of Oxford.

AUTHOR CONTRIBUTIONS

J.W. and J.L. designed the research; J.W. performed research and analyzed data; T.Y., A.D.H, and S.T. provided mimetic compound 3; S.T., J.W., and J.L. revised the paper.

DECLARATION OF INTERESTS

The authors declare no competing interests.

Received: August 24, 2022
Revised: November 7, 2022
Accepted: December 22, 2022
Published: January 18, 2023

REFERENCES

1. Jakes, R., Spillantini, M.G., and Goedert, M. (1994). Identification of two distinct synucleins from human brain. FEBS Lett. *345*, 27–32.
2. Davidson, W.S., Jonas, A., Clayton, D.F., and George, J.M. (1998). Stabilization of α-synuclein secondary structure upon binding to synthetic membranes. J. Biol. Chem. *273*, 9443–9449.
3. Rovere, M., Sanderson, J.B., Fonseca-Ornelas, L., Patel, D.S., and Bartels, T. (2018). Refolding of helical soluble α-synuclein through transient interaction with lipid interfaces. FEBS Lett. *592*, 1464–1472.
4. Eliezer, D., Kutluay, E., Bussell, R., Jr., and Browne, G. (2001). Conformational properties of α-synuclein in its free and lipid-associated states. J. Mol. Biol. *307*, 1061–1073.
5. Chen, M., Margittai, M., Chen, J., and Langen, R. (2007). Investigation of α-synuclein fibril structure by site-directed spin labeling. J. Biol. Chem. *282*, 24970–24979.
6. Comellas, G., Lemkau, L.R., Zhou, D.H., George, J.M., and Rienstra, C.M. (2012). Structural intermediates during α-synuclein fibrillogenesis on phospholipid vesicles. J. Am. Chem. Soc. *134*, 5090–5099.
7. Perrin, R.J., Woods, W.S., Clayton, D.F., and George, J.M. (2000). Interaction of human α-synuclein and Parkinson's disease variants with phospholipids: structural analysis using site-directed mutagenesis. J. Biol. Chem. *275*, 34393–34398.
8. van Rooijen, B.D., Claessens, M.M.A.E., and Subramaniam, V. (2008). Membrane binding of oligomeric α-synuclein depends on bilayer charge and packing. FEBS Lett. *582*, 3788–3792.
9. Ghio, S., Kamp, F., Cauchi, R., Giese, A., and Vassallo, N. (2016). Interaction of α-synuclein with biomembranes in Parkinson's disease—role of cardiolipin. Prog. Lipid Res. *61*, 73–82.
10. Gurnev, P.A., Yap, T.L., Pfefferkorn, C.M., Rostovtseva, T.K., Berezhkovskii, A.M., Lee, J.C., Parsegian, V.A., and Bezrukov, S.M. (2014). Alpha-synuclein lipid-dependent membrane binding and translocation through the α-hemolysin channel. Biophys. J. *106*, 556–565. https://doi.org/10.1016/j.bpj.2013.12.028.
11. Pacheco, C., Aguayo, L.G., and Opazo, C. (2012). An extracellular mechanism that can explain the neurotoxic effects of α-synuclein aggregates in the brain. Front. Physiol. *3*, 297.
12. Wu, J., Blum, T.B., Farrell, D.P., DiMaio, F., Abrahams, J.P., and Luo, J. (2021). Cryo-electron microscopy imaging of Alzheimer's amyloid-beta 42 oligomer displayed on a functionally and structurally relevant scaffold. Angew Chem. Int. Ed. Engl. *60*, 18680–18687.
13. Wu, J., Cao, C., Loch, R.A., Tiiman, A., and Luo, J. (2020). Single-molecule studies of amyloid proteins: from biophysical properties to diagnostic perspectives. Q. Rev. Biophys. *53*, e12.
14. Pandey, A.P., Haque, F., Rochet, J.-C., and Hovis, J.S. (2009). Clustering of α-synuclein on supported lipid bilayers: role of anionic lipid, protein, and divalent ion concentration. Biophys. J. *96*, 540–551.
15. Ugalde, C.L., Lawson, V.A., Finkelstein, D.I., and Hill, A.F. (2019). The role of lipids in α-synuclein misfolding and neurotoxicity. J. Biol. Chem. *294*, 9016–9028. https://doi.org/10.1074/jbc.REV119.007500.
16. Middleton, E.R., and Rhoades, E. (2010). Effects of curvature and composition on α-synuclein binding to lipid vesicles. Biophys. J. *99*, 2279–2288. https://doi.org/10.1016/j.bpj.2010.07.056.
17. Ouberai, M.M., Wang, J., Swann, M.J., Galvagnion, C., Guilliams, T., Dobson, C.M., and Welland, M.E. (2013). α-Synuclein senses lipid packing defects and induces lateral expansion of lipids leading to membrane remodeling. J. Biol. Chem. *288*, 20883–20895.
18. Burré, J., Sharma, M., and Südhof, T.C. (2015). Definition of a molecular pathway mediating α-synuclein neurotoxicity. J. Neurosci. *35*, 5221–5232. https://doi.org/10.1523/jneurosci.4650-14.2015.
19. Ugalde, C.L., Finkelstein, D.I., Lawson, V.A., and Hill, A.F. (2016). Pathogenic mechanisms of prion protein, amyloid-β and α-synuclein misfolding: the prion concept and neurotoxicity of protein oligomers. J. Neurochem. *139*, 162–180. https://doi.org/10.1111/jnc.13772.
20. Hozumi, I., Hasegawa, T., Honda, A., Ozawa, K., Hayashi, Y., Hashimoto, K., Yamada, M., Koumura, A., Sakurai, T., Kimura, A., et al. (2011). Patterns of levels of biological metals in CSF differ among neurodegenerative diseases. J. Neurol. Sci. *303*, 95–99.
21. Dexter, D.T., Wells, F.R., Lees, A.J., Agid, F., Agid, Y., Jenner, P., and Marsden, C.D. (1989). Increased nigral iron content and alterations in other metal ions occurring in brain in Parkinson's disease. J. Neurochem. *52*, 1830–1836.
22. Barnham, K.J., and Bush, A.I. (2008). Metals in Alzheimer's and Parkinson's diseases. Curr. Opin. Chem. Biol. *12*, 222–228.
23. Deas, E., Cremades, N., Angelova, P.R., Ludtmann, M.H.R., Yao, Z., Chen, S., Horrocks, M.H., Banushi, B., Little, D., Devine, M.J., et al. (2016). Alpha-synuclein oligomers interact with metal ions to induce oxidative stress and neuronal death in Parkinson's disease. Antioxidants Redox Signal. *24*, 376–391.
24. Binolfi, A., Rasia, R.M., Bertoncini, C.W., Ceolin, M., Zweckstetter, M., Griesinger, C., Jovin, T.M., and Fernández, C.O. (2006). Interaction of α-synuclein with divalent metal ions reveals key differences: a link between structure, binding specificity and fibrillation enhancement. J. Am. Chem. Soc. *128*, 9893–9901.
25. Deas, E., Cremades, N., Angelova, P.R., Ludtmann, M.H.R., Yao, Z., Chen, S., Horrocks, M.H., Banushi, B., Little, D., Devine, M.J., et al. (2016). Alpha-synuclein oligomers interact with metal ions to induce oxidative stress and neuronal death in Parkinson's disease. Antioxidants Redox Signal. *24*, 376–391. https://doi.org/10.1089/ars.2015.6343.
26. Rasia, R.M., Bertoncini, C.W., Marsh, D., Hoyer, W., Cherny, D., Zweckstetter, M., Griesinger, C., Jovin, T.M., and Fernández, C.O. (2005). Structural characterization of copper (II) binding to α-synuclein: insights into the bioinorganic chemistry of Parkinson's disease. Proc. Natl. Acad. Sci. USA *102*, 4294–4299.
27. Houghtaling, J., List, J., and Mayer, M. (2018). Nanopore-based, rapid characterization of individual amyloid particles in solution: concepts, challenges, and prospects. Small *14*, 1802412.
28. Wang, H.-Y., Ying, Y.-L., Li, Y., Kraatz, H.-B., and Long, Y.-T. (2011). Nanopore analysis of β-amyloid peptide aggregation transition induced by small molecules. Anal. Chem. *83*, 1746–1752.
29. Wang, H.-Y., Gu, Z., Cao, C., Wang, J., and Long, Y.-T. (2013). Analysis of a single α-synuclein fibrillation by the interaction with a protein nanopore. Anal. Chem. *85*, 8254–8261.
30. Asandei, A., Iftemi, S., Mereuta, L., Schiopu, I., and Luchian, T. (2014). Probing of various physiologically relevant metals: amyloid-β peptide interactions with a lipid membrane-immobilized protein nanopore. J. Membr. Biol. *247*, 523–530.
31. Movileanu, L., Schmittschmitt, J.P., Scholtz, J.M., and Bayley, H. (2005). Interactions of peptides with a protein pore. Biophys. J. *89*, 1030–1045.
32. Mereuta, L., Schiopu, I., Asandei, A., Park, Y., Hahm, K.-S., and Luchian, T. (2012). Protein nanopore-based, single-molecule exploration of copper binding to an antimicrobial-derived, histidine-containing chimera peptide. Langmuir *28*, 17079–17091.
33. Song, L., Hobaugh, M.R., Shustak, C., Cheley, S., Bayley, H., and Gouaux, J.E. (1996). Structure of staphylococcal alpha-hemolysin, a heptameric transmembrane pore. Science *274*, 1859–1866. https://doi.org/10.1126/science.274.5294.1859.
34. Ferreon, A.C.M., Gambin, Y., Lemke, E.A., and Deniz, A.A. (2009). Interplay of α-synuclein binding and conformational switching probed by single-molecule fluorescence. Proc. Natl. Acad. Sci. USA *106*, 5645–5650. https://doi.org/10.1073/pnas.0809232106.
35. Tavassoly, O., Nokhrin, S., Dmitriev, O.Y., and Lee, J.S. (2014). Cu(II) and dopamine bind to α-synuclein and cause large conformational changes. FEBS J. *281*, 2738–2753. https://doi.org/10.1111/febs.12817.
36. Rodriguez-Larrea, D., and Bayley, H. (2014). Protein co-translocational unfolding depends on the direction of pulling. Nat. Commun. *5*, 4841. https://doi.org/10.1038/ncomms5841.
37. Rodriguez-Larrea, D., and Bayley, H. (2013). Multistep protein unfolding during nanopore translocation. Nat. Nanotechnol. *8*, 288–295. https://doi.org/10.1038/nnano.2013.22.
38. Zhu, J., Hu, G., and Xuan, X. (2012). Electrokinetic particle entry into microchannels. Electrophoresis *33*, 916–922.
39. Lashuel, H.A., Overk, C.R., Oueslati, A., and Masliah, E. (2013). The many faces of

α-synuclein: from structure and toxicity to therapeutic target. Nat. Rev. Neurosci. *14*, 38–48. https://doi.org/10.1038/nrn3406.

40. Davidson, W.S., Jonas, A., Clayton, D.F., and George, J.M. (1998). Stabilization of alpha-synuclein secondary structure upon binding to synthetic membranes. J. Biol. Chem. *273*, 9443–9449. https://doi.org/10.1074/jbc.273.16.9443.

41. Epand, R.F., Maloy, L., Ramamoorthy, A., and Epand, R.M. (2010). Amphipathic helical cationic antimicrobial peptides promote rapid formation of crystalline states in the presence of phosphatidylglycerol: lipid clustering in anionic membranes. Biophys. J. *98*, 2564–2573.

42. Paterson, D.J., Tassieri, M., Reboud, J., Wilson, R., and Cooper, J.M. (2017). Lipid topology and electrostatic interactions underpin lytic activity of linear cationic antimicrobial peptides in membranes. Proc. Natl. Acad. Sci. USA *114*, E8324–E8332.

43. Magzoub, M., Kilk, K., Eriksson, L.E., Langel, Ü., and Gräslund, A. (2001). Interaction and structure induction of cell-penetrating peptides in the presence of phospholipid vesicles. Biochim. Biophys. Acta *1512*, 77–89.

44. Jobin, M.-L., Bonnafous, P., Temsamani, H., Dole, F., Grélard, A., Dufourc, E.J., and Alves, I.D. (2013). The enhanced membrane interaction and perturbation of a cell penetrating peptide in the presence of anionic lipids: toward an understanding of its selectivity for cancer cells. Biochim. Biophys. Acta *1828*, 1457–1470.

45. Binder, H., and Lindblom, G. (2004). A molecular view on the interaction of the trojan peptide penetratin with the polar interface of lipid bilayers. Biophys. J. *87*, 332–343.

46. Deol, S.S., Domene, C., Bond, P.J., and Sansom, M.S.P. (2006). Anionic phospholipid interactions with the potassium channel KcsA: simulation studies. Biophys. J. *90*, 822–830.

47. Rosen, C.B., Rodriguez-Larrea, D., and Bayley, H. (2014). Single-molecule site-specific detection of protein phosphorylation with a nanopore. Nat. Biotechnol. *32*, 179–181. https://doi.org/10.1038/nbt.2799.

48. Maglia, G., Restrepo, M.R., Mikhailova, E., and Bayley, H. (2008). Enhanced translocation of single DNA molecules through alpha-hemolysin nanopores by manipulation of internal charge. Proc. Natl. Acad. Sci. USA *105*, 19720–19725. https://doi.org/10.1073/pnas.0808296105.

49. Hu, R., Diao, J., Li, J., Tang, Z., Li, X., Leitz, J., Long, J., Liu, J., Yu, D., and Zhao, Q. (2016). Intrinsic and membrane-facilitated α-synuclein oligomerization revealed by label-free detection through solid-state nanopores. Sci. Rep. *6*, 20776. https://doi.org/10.1038/srep20776.

50. Wang, H.Y., Ying, Y.L., Li, Y., Kraatz, H.B., and Long, Y.T. (2011). Nanopore analysis of β-amyloid peptide aggregation transition induced by small molecules. Anal. Chem. *83*, 1746–1752. https://doi.org/10.1021/ac1029874.

51. Meyer, N., Arroyo, N., Janot, J.M., Lepoitevin, M., Stevenson, A., Nemeir, I.A., Perrier, V., Bougard, D., Belondrade, M., Cot, D., et al. (2021). Detection of amyloid-β fibrils using track-etched nanopores: effect of geometry and crowding. ACS Sens. *6*, 3733–3743. https://doi.org/10.1021/acssensors.1c01523.

52. Stefureac, R.I., Madampage, C.A., Andrievskaia, O., and Lee, J.S. (2010). Nanopore analysis of the interaction of metal ions with prion proteins and peptidesThis paper is one of a selection of papers published in this special issue entitled "Canadian Society of Biochemistry, Molecular & Cellular Biology 52nd Annual Meeting — protein Folding: principles and Diseases" and has undergone the Journal's usual peer review process. Biochem. Cell. Biol. *88*, 347–358. https://doi.org/10.1139/O09-176.

53. Wang, H., Mörman, C., Sternke-Hoffmann, R., Huang, C.-Y., Prota, A., Ma, P., and Luo, J. (2022). Cu2+ ions modulate the interaction between α-synuclein and lipid membranes. J. Inorg. Biochem. *236*, 111945. https://doi.org/10.1016/j.jinorgbio.2022.111945.

54. Feng, J., Martin-Baniandres, P., Booth, M.J., Veggiani, G., Howarth, M., Bayley, H., and Rodriguez-Larrea, D. (2020). Transmembrane protein rotaxanes reveal kinetic traps in the refolding of translocated substrates. Commun. Biol. *3*, 159. https://doi.org/10.1038/s42003-020-0840-5.

55. Stoddart, D., Heron, A.J., Mikhailova, E., Maglia, G., and Bayley, H. (2009). Single-nucleotide discrimination in immobilized DNA oligonucleotides with a biological nanopore. Proc. Natl. Acad. Sci. USA *106*, 7702–7707. https://doi.org/10.1073/pnas.0901054106.

56. Ding, Y., and Kanavarioti, A. (2016). Single pyrimidine discrimination during voltage-driven translocation of osmylated oligodeoxynucleotides via the α-hemolysin nanopore. Beilstein J. Nanotechnol. *7*, 91–101. https://doi.org/10.3762/bjnano.7.11.

57. van Rooijen, B.D., Claessens, M.M.A.E., and Subramaniam, V. (2009). Lipid bilayer disruption by oligomeric alpha-synuclein depends on bilayer charge and accessibility of the hydrophobic core. Biochim. Biophys. Acta *1788*, 1271–1278. https://doi.org/10.1016/j.bbamem.2009.03.010.

58. Kjaer, L., Giehm, L., Heimburg, T., and Otzen, D. (2009). The influence of vesicle size and composition on alpha-synuclein structure and stability. Biophys. J. *96*, 2857–2870. https://doi.org/10.1016/j.bpj.2008.12.3940.

59. Stöckl, M., Fischer, P., Wanker, E., and Herrmann, A. (2008). α-Synuclein selectively binds to anionic phospholipids embedded in liquid-disordered domains. J. Mol. Biol. *375*, 1394–1404. https://doi.org/10.1016/j.jmb.2007.11.051.

60. Moons, R., Konijnenberg, A., Mensch, C., Van Elzen, R., Johannessen, C., Maudsley, S., Lambeir, A.-M., and Sobott, F. (2020). Metal ions shape α-synuclein. Sci. Rep. *10*, 16293. https://doi.org/10.1038/s41598-020-73207-9.

61. Bavinton, C.E., Sternke-Hoffmann, R., Yamashita, T., Knipe, P.C., Hamilton, A.D., Luo, J., and Thompson, S. (2022). Rationally designed helical peptidomimetics disrupt alpha–synuclein fibrillation. Chem. Commun. *58*, 5132–5135.

62. Croke, R.L., Patil, S.M., Quevreaux, J., Kendall, D.A., and Alexandrescu, A.T. (2011). NMR determination of pKa values in α-synuclein. Protein Sci. *20*, 256–269.

63. Peacock, H., Luo, J., Yamashita, T., Luccarelli, J., Thompson, S., and Hamilton, A.D. (2016). Non-covalent S··· O interactions control conformation in a scaffold that disrupts islet amyloid polypeptide fibrillation. Chem. Sci. *7*, 6435–6439.

64. Cappai, R., Leck, S.-L., Tew, D.J., Williamson, N.A., Smith, D.P., Galatis, D., Sharples, R.A., Curtain, C.C., Ali, F.E., Cherny, R.A., et al. (2005). Dopamine promotes α-synuclein aggregation into SDS-resistant soluble oligomers via a distinct folding pathway. Faseb. J. *19*, 1377–1379. https://doi.org/10.1096/fj.04-3437fje.

65. Planchard, M.S., Exley, S.E., Morgan, S.E., and Rangachari, V. (2014). Dopamine-induced α-synuclein oligomers show self-and cross-propagation properties. Protein Sci. *23*, 1369–1379.

66. Fischer, A.F., and Matera, K.M. (2015). Stabilization of alpha-synuclein oligomers in vitro by the neurotransmitters, dopamine and norepinephrine: the effect of oxidized catecholamines. Neurochem. Res. *40*, 1341–1349.

67. Mor, D.E., Tsika, E., Mazzulli, J.R., Gould, N.S., Kim, H., Daniels, M.J., Doshi, S., Gupta, P., Grossman, J.L., Tan, V.X., et al. (2017). Dopamine induces soluble α-synuclein oligomers and nigrostriatal degeneration. Nat. Neurosci. *20*, 1560–1568.

68. Wang, Y., Wang, Y., Du, X., Yan, S., Zhang, P., Chen, H.-Y., and Huang, S. (2019). Electrode-free nanopore sensing by DiffusiOptoPhysiology. Sci. Adv. *5*, eaar3309.

69. Baaken, G., Sondermann, M., Schlemmer, C., Rühe, J., and Behrends, J.C. (2008). Planar microelectrode-cavity array for high-resolution and parallel electrical recording of membrane ionic currents. Lab Chip *8*, 938–944.